

# Imaging the He<sub>2</sub> quantum halo state using a free electron laser

S. Zeller<sup>a,1</sup>, M. Kunitski<sup>a</sup>, J. Voigtsberger<sup>a</sup>, A. Kalinin<sup>a</sup>, A. Schottelius<sup>a</sup>, C. Schober<sup>a</sup>, M. Waitz<sup>a</sup>, H. Sann<sup>a</sup>, A. Hartung<sup>a</sup>, T. Bauer<sup>a</sup>, M. Pitzer<sup>a</sup>, F. Trinter<sup>a</sup>, C. Gohl<sup>a</sup>, C. Janke<sup>a</sup>, M. Richter<sup>a</sup>, G. Kastirke<sup>a</sup>, M. Weller<sup>a</sup>, A. Czasch<sup>a</sup>, M. Kitzler<sup>b</sup>, M. Braune<sup>c</sup>, R. E. Grisenti<sup>a,d</sup>, W. Schöllkopf<sup>e</sup>, L. Ph. H. Schmidt<sup>a</sup>, M. Schöffler<sup>a</sup>, J. B. Williams<sup>f</sup>, T. Jahnke<sup>a</sup>, and R. Dörner<sup>a,1</sup>

<sup>a</sup>Institut für Kernphysik, Goethe-Universität Frankfurt, 60438 Frankfurt am Main, Germany; <sup>b</sup>Photonics Institute, Vienna University of Technology, Gußhausstraße 27, 1040 Vienna, Austria; <sup>c</sup>Deutsches Elektronen-Synchrotron DESY, Notkestraße 85, 22607 Hamburg, Germany; <sup>d</sup>GSF Helmholtz Centre for Heavy Ion Research, Planckstraße 1, 64291 Darmstadt, Germany; <sup>e</sup>Department of Molecular Physics, Fritz-Haber-Institut, Faradayweg 4-6, 14195 Berlin, Germany; <sup>f</sup>Department of Physics, University of Nevada, 1664 N. Virginia Street, Reno, NV 89557, USA

This manuscript was compiled on June 30, 2016

**Quantum tunneling is a ubiquitous phenomenon in nature and crucial for many technological applications. It allows quantum particles to reach regions in space which are energetically not accessible according to classical mechanics. In this “tunneling region”, the particle density is known to decay exponentially. This behavior is universal across all energy scales from nuclear physics to chemistry and solid state systems. While typically only a small fraction of a particle wavefunction extends into the tunneling region, we here present an extreme quantum system: a gigantic molecule consisting of two helium atoms, with an 80% probability that its two nuclei will be found in this classical forbidden region. This allows for the first time to directly image the exponentially decaying density of a tunneling particle, which we achieved for over two orders of magnitude. This shows one of the few features of our world, which is truly universal: the probability to find one of the constituents of bound matter far away is never zero but decreases exponentially. The results were obtained by Coulomb explosion imaging using a free electron laser and furthermore yield He<sub>2</sub>'s binding energy of  $151.9 \pm 13.3$  neV, which is in agreement with most recent calculations.**

Atomic Physics | Atomic and Molecular Clusters

**A**ttractive forces allow particles to condense into stable bound systems such as molecules or nuclei with a ground state and (in most cases) energetically excited bound states, as sketched in Fig. 1. Classical particles situated in such a binding potential oscillate back and forth between two turning points. The regions beyond these points are inaccessible for a classical particle due to a lack of energy. Quantum particles, however, can penetrate into the potential barrier by a phenomenon known as “tunneling”. Tunneling is omnipresent in nature and occurs on all energy scales from MeV in nuclear physics, to eV in molecules and solids, and to neV in optical lattices. For bound matter the fraction of the probability density distribution in this classically forbidden region is usually small. For shallow short range potentials this can change dramatically: upon decreasing the potential depth excited states are expelled one after the other as they become unbound (transition from Fig. 1A to B). A further decrease of the potential depth effects the ground state as well, as more and more of its wavefunction expands into the tunneling region (Fig. 1C/D). Consequently, at the threshold (i.e. in the limit of vanishing binding energy) the size of the quantum system expands to infinity. For short range potentials this expansion is accompanied by the fact that the system becomes less “classical” and more quantum-like. Systems existing near that threshold (and therefore being dominated by the tunneling part of their

wavefunction) are called “quantum halo states” [1]. These are, for example, known from nuclear physics where <sup>11</sup>Be and <sup>11</sup>Li form halo states [2–4].

One of the most extreme examples of such a quantum halo state can be found in the realm of atomic physics: the helium dimer (He<sub>2</sub>). It is bound by the van der Waals force only and the He-He interaction potential (see Fig. 1D) has a minimum of about 1 meV at an internuclear distance of about 3 Å (0.947 meV / 2.96 Å[5]). For a long time it was controversial whether already the zero point energy of the helium dimer is larger than the depth of the potential well and thus whether the helium dimer exists as a stable molecule at all. While <sup>3</sup>He<sup>4</sup>He is indeed unbound because of its bigger zero point energy, stable <sup>4</sup>He<sub>2</sub> was finally found experimentally in 1993/94 [6, 7]. It turns out, that He<sub>2</sub> has no bound excited rotational states as already the centrifugal force associated with 1ħ of angular momentum leads to dissociation. Experiments using matter wave diffraction confirmed the halo character of He<sub>2</sub> by measuring a mean value of the internuclear distance of 52 Å[8]. This is in agreement with some theoretical predictions, but in conflict with the most recent calculations[5]. Resolving this conflict is of importance also for the planned redefinition of the Kelvin, unit of thermodynamic temperature, in terms of the Boltzmann constant [9]. Thermometry today uses theoretical

## Significance Statement

In bound matter on all length scales from nuclei to molecules to macroscopic solid objects most of the density of the bound particles is within the range of the interaction potential which holds the system together. Quantum halos on the contrary are a type of matter where the particle density is mostly outside the range of the interaction potential in the tunneling region of the potential. Few examples of these fascinating systems are known in nuclear and molecular physics. The conceptually simplest halo system is made of only two particles. Here we experimentally image the wavefunction of the He<sub>2</sub> quantum halo. It shows the predicted exponential shape of a tunneling wavefunction.

S.Z., M.K., J.V. and T.J. designed and constructed the experimental setup. S.Z., J.V., A.K., A.S., C.S., M.W., H.S., A.H., T.B., M.P., F.T., C.G., C.J., M.R., G.K., M.W., L.P.H.S., M.S., J.B.W., T.J. and R.D. performed the experiment at the FEL. A.C. and T.B. contributed to the online data analysis. M.B. provided technical support at the FEL. R.E.G., A.K., S.Z. and W.S. developed the jet diffraction system. S.Z., T.J. and R.D. analyzed the data and wrote the manuscript. All authors discussed the results and commented on the manuscript.

<sup>2</sup>Correspondence and requests for materials should be addressed to S.Z. (zeller[at]atom.uni-frankfurt.de) or R.D. (doerner[at]atom.uni-frankfurt.de)

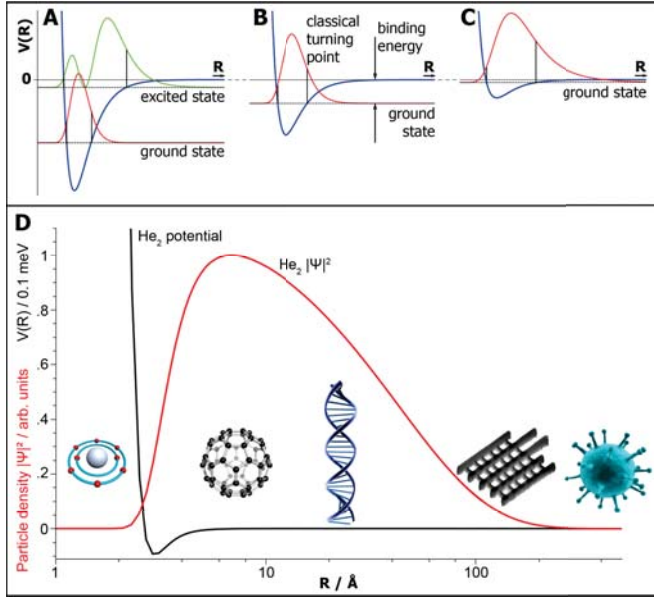


**Fig. 1.** A shallow short range potential holding a ground and an excited state (A). As the potential depth decreases (B) the excited state becomes unbound, leaving only the ground state. Further decrease (C) leads to the particle probability density distribution leaking more into the classically forbidden region. In the extreme case of the helium dimer (D) (note the logarithmic R-scale) this effect allows the wavefunction to extend to sizes of fullerenes, the diameter of DNA and even small viruses ( $\text{He}_2$  potential and wavefunction taken from [5]): while the classical turning point is located at 13.6 Å the overall wavefunction extends to more than 200 Å.

values for the thermal conductivity and viscosity of helium. Those properties are based on the same He-He interaction potential used to calculate the  $\text{He}_2$  binding energy, which was shown to be incompatible with previous experiments[8, 10] (see [11] for a more detailed discussion).

At the same time its quantum halo character makes  $\text{He}_2$  a prime candidate for visualizing the predicted universal exponential decrease of a tunneling wavefunction in an experiment by triggering a Coulomb explosion with a free electron laser (FEL).

## Results

In the corresponding experiment presented here, helium clusters were produced by expanding cooled helium gas through a 5  $\mu\text{m}$  nozzle. By matter wave diffraction a pure helium dimer beam was separated from the lighter monomers and heavier clusters[6]. In two experimental campaigns both atoms of the dimer were then singly ionized employing either single photon ionization using photons provided by a free electron laser (FLASH, <100 fs, 18.5 nm) or tunnel ionization using a strong ultrashort laser field (Ti:Sa laser, Dragon KMLabs, 780 nm). In both cases the ionization of the two atoms occurs fast compared to the nuclear motion, thus triggering an instantaneous Coulomb explosion of the repelling ionized particles. The Coulomb explosion converts the potential energy of the two ions located at an internuclear distance  $R$  into a released kinetic energy (KER) according to

$$R = \frac{1}{KER}. \quad [1]$$

By recording a large number of Coulomb explosion events, via cold target recoil ion momentum spectroscopy

(COLTRIMS)[12–14], a distribution of measured distances  $R$  (as shown in Fig. 2A) is obtained. It represents a direct measurement of the square of the helium dimer wavefunction  $|\Psi|^2$ . The classically allowed part of  $|\Psi|^2$  provides a cross-check for our measurement as it falls off steeply at the inner turning point of the helium dimer potential and theoretical calculations agree well on the location of the turning point. A comparison of our measured probability density distribution close to the inner turning point and some theoretical predictions are shown in Fig. 2B. Here two exemplary theoretical curves[5, 15] are depicted along with a measurement conducted at our Ti:Sa laser as it provides very high resolution and statistics for small internuclear distances.

The classically forbidden part of  $|\Psi|^2$  is shown in Fig. 2C on a logarithmic scale. For internuclear distances larger than 30 Å the helium dimer potential is two orders of magnitude smaller than the predicted ground state binding energy and thus can safely be approximated to zero. Accordingly, the wavefunction is approximated in this region by the solution of the Schrödinger equation below a steplike barrier, which is given by

$$\Psi(R) \propto e^{-\sqrt{\frac{2m}{\hbar^2} E_{bind}} R}. \quad [2]$$

As the mass  $m$  and Planck's constant  $\hbar$  are fixed, the only variable defining the slope of the exponential decay is the binding energy  $E_{bind}$ . Therefore the binding energy can be extracted from the measurement by an exponential fit to the pair-distance distribution, as depicted in Fig. 2C. From the fit we obtain a helium dimer binding energy of  $151.9 \pm 13.3$  neV (see methods for discussion of errors and corrections to equation 2).

## Discussion

The theoretical value for the binding energy was under dispute for many years[16–19]. Predictions range from 44.8 neV[17] to 161.7 neV[20]. Recently calculations became available which include quantum electrodynamical effect, relativistic effects and go beyond the Born Oppenheimer approximation. These supposedly most precise calculations predict a binding energy of  $139.2 \pm 2.9$  neV[5], which is in disagreement with the most recent experimental value of  $94.8 +25.9/-17.2$  neV obtained in pioneering experiments by evaluating matterwave diffraction patterns and relying on a detailed theoretical modelling of the interaction of the dimer with the grating surface[8]. The present value of  $151.9 \pm 13.3$  neV is in good agreement with the prediction of Przybytek et al.[5] ( $139.2 \pm 2.9$  neV) and in clear disagreement with the predictions from some He-He interaction potentials, including the popular TTY[18] and LM2M2[21] potentials yielding 114 and 113 neV, respectively. The helium dimer is a remarkable example of a system existing predominantly in the quantum mechanical tunneling regime. We were able to reveal the full shape of the wavefunction experimentally. The measured data confirms the universal exponential behavior of wavefunctions under a potential barrier on unprecedented scales and yields a revised experimental value for the binding energy of the helium dimer, which has been under dispute for more than 20 years.

## Materials and Methods

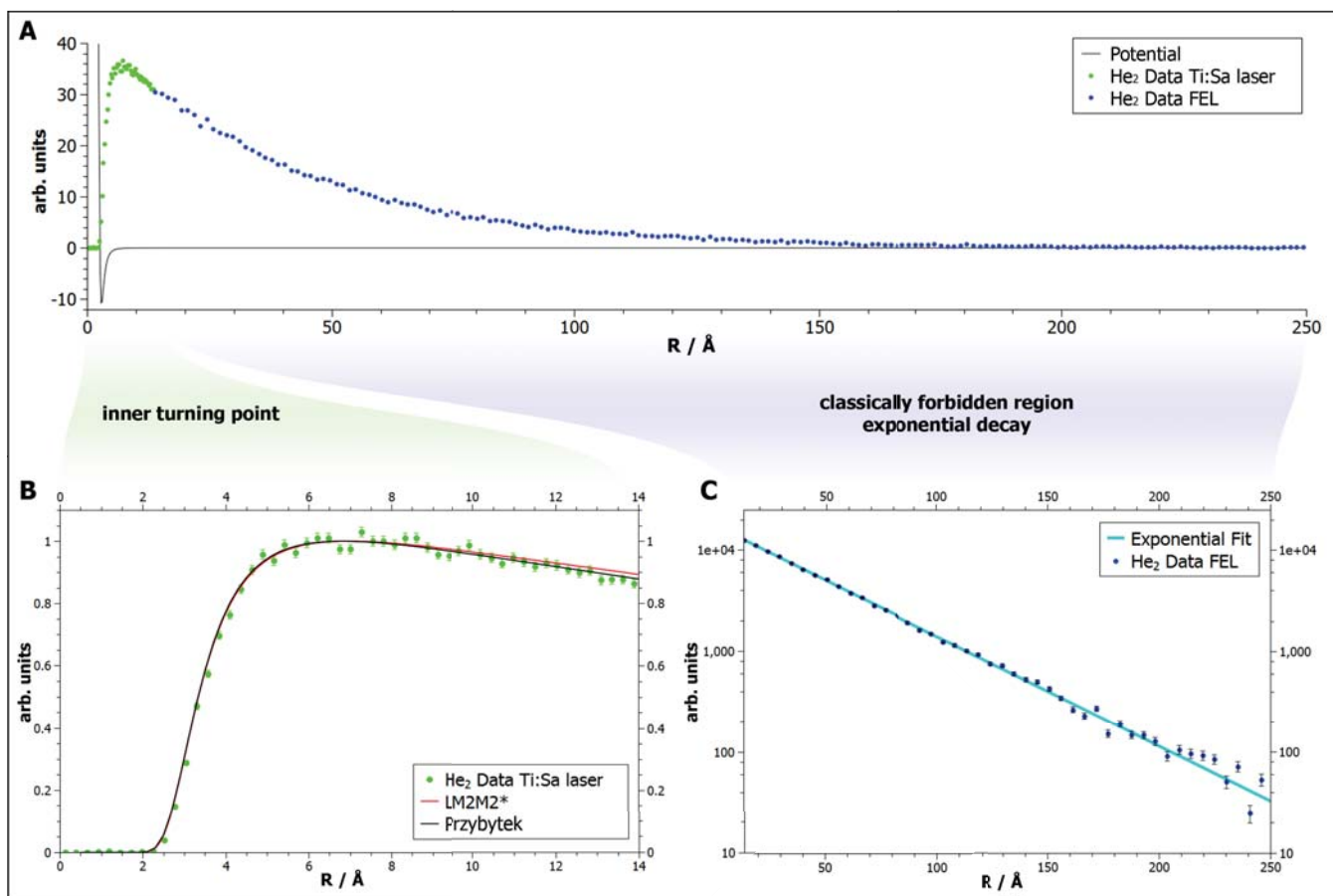


**Fig. 2.** Measurement of the helium dimer wavefunction (A). Two detailed views show the important features of this quantum system: The region of the inner turning point (B) is in agreement with theoretical predictions LM2M2\*[15] and Przybytek[5], and the exponential decay in the classical forbidden region (C). A helium dimer binding energy of  $151.9 \pm 13.3$  neV is obtained from the exponential slope. The electron recoil has to be taken into account to conclude from the slope shown in C to the value of the binding energy (see text for details).

**Dimer preparation and detection.** A mixture of helium clusters was produced by expanding gaseous helium through a  $5 \mu\text{m}$  nozzle. The nozzle was cooled down to 8 K and a driving pressure of 450 mbar abs. was applied to maximize the dimer content in the molecular beam[22]. To obtain a pure helium dimer target beam we made use of matter wave diffraction. All clusters have the same velocity but can be sorted by mass as their diffraction angle behind a transmission grating (100 nm period) depends on their de Broglie wavelengths ( $\lambda = h/mv$ , with Planck's constant  $h$ , mass  $m$  and velocity  $v$ ). That way only dimers reach the laser focus while the dominant fraction of atomic helium as well as the share of helium trimers present at the chosen gas expansion conditions get deflected away from the ionization region. Figure 3 shows a schematic of the setup.

The two atoms constituting the dimer get singly ionized in the focus either via photoeffect (free electron laser, FLASH, 18.5 nm) or via tunnelionization (Ti:Sa laser, Dragon KMLabs, 780 nm). The two positively charged ions repel each other, resulting in a Coulomb explosion. The ionic momenta acquired in this explosion were measured by cold target recoil ion momentum spectroscopy (COLTRIMS). A homogeneous electric field of 4.41 V/cm (at free electron laser) / 3.09 V/cm (at Ti:Sa laser) guides the ions to the detector. It measures time-of-flight and position of impact using micro channel plates (MCP) and delay line anodes[12]. With known electric fields, ion masses, ion charges and distance from focus to detector of 39 mm the initial momentum vector of the ions and thus the KER can be reconstructed.

**Detector calibration.** The binding energy of the helium dimer is derived from the measured KER. Therefore a precise energy cali-

bration is needed. The crucial parameters for this calibration are the absolute value of the electric field in the spectrometer and the position calibration of the detector. The electric field was obtained by measuring the kinetic energy release spectrum of the  $\text{N}_2$  breakup which provides very narrow peaks. Transitions from  $\text{D}^3\Pi_g$  and  $\text{D}^1\Sigma_u^+$  into continuum could be identified and met reference measurements[23] with a mean relative deviation of 0.054%. This yielded the calibration of the momentum component along the time-of-flight direction of the spectrometer.

The position calibration was done by comparing the momentum component in the time-of-flight direction with the ones perpendicular to it. For this purpose we performed two calibration measurements with isotropic dissociation channels ( $\text{N}_2\text{O}$  /  $\text{Ne}_2$ ). Most relevant, due to energetic proximity to the helium dimer breakup, is the  $\text{N}_2\text{O}$  channel at 0.16 eV KER with a mean relative deviation of 6.2%, while additional channels yield a smaller deviation with 0.62% ( $\text{N}_2\text{O}$  at 0.36 eV) and 0.15% ( $\text{Ne}_2$  at 4.4 eV).

For the experiment at FLASH, despite excellent vacuum conditions ( $8 \cdot 10^{-12}$  mbar), an average of about 50 ions were collected for every FEL pulse. The majority of ions were charged hydrogen atoms or molecules with short times-of-flight, which could be gated out by software during data acquisition prior to writing to the hard drive. Nevertheless the MCP endured constant stress which led to a drop in detection efficiency in the center of the detector. The detection efficiency was corrected to its normal level using a residual gas calibration measurement with a Gaussian shaped correction function containing a 5.5% uncertainty. This leads to  $\pm 1$  neV uncertainty on the binding energy. In addition random coincidences from ionizations of two independent helium ions from the residual gas were subtracted. The error resulting from this background subtraction is

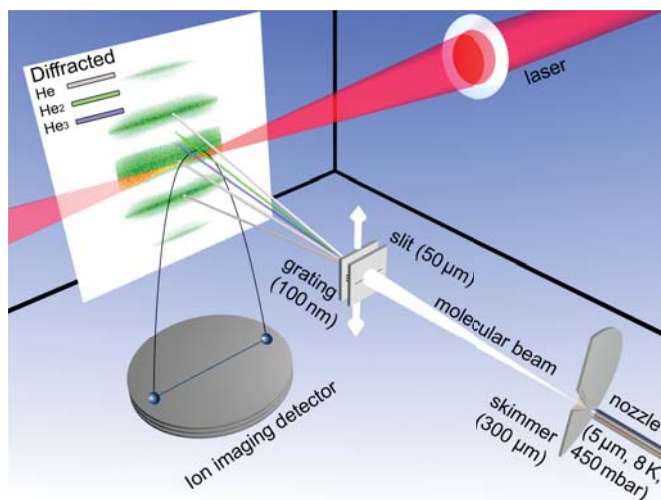


**Fig. 3.** Overlap between laser focus and a pure helium dimer beam, created by a molecular beam diffracted at a nanograting. Distances between the beam elements were as follows: nozzle to skimmer 14 mm, skimmer to slit 332 mm, slit to grating 30 mm, grating to focus 491 mm. The focus diameter was about  $20 \mu\text{m}$ .

small in comparison to errors discussed above ( $\pm 0.4 \text{ neV}$ ).

**Binding energy derivation.** The solution to the Schrödinger equation in the region below a potential barrier is an exponential decay function (equation 2). The helium dimer binding energy has been extracted from the experimental data by applying an exponential fit to the reconstructed pair-distance distribution (50 a.u. to 300 a.u.). We excluded breakups recorded in the detector plane (with a tolerance of  $\pm 33.5^\circ$ ) as indistinguishable background and potentially deadline effects compromised the data here.

To image the exact shape of the probability density distribution by Coulomb explosion imaging the ionization probability has to be independent of the internuclear distance. Two consecutive tunnel ionization steps can be influenced by enhanced ionization[24], an effect which depends on the internuclear distance. The steep rise of the probability density at the inner turning point is not very sensitive to this effect and could consequently be imaged by our experiment with an 800 nm laser pulse, which has superior statistics compared to the FEL experiment (see Fig. 2). For the exponential region of the probability density we aim for a high precision determination of the slope. We therefore used photons from the free electron laser FLASH to ionize both atoms of the dimer by single photon absorption. Compared to an 800 nm laser pulse this has the additional advantage that the electron energy, and thus the recoil of the electrons onto the nuclei, is much better controlled and has an upper threshold.

**Electron recoil correction.** The initial ion energy during the Coulomb breakup has to be either zero or well defined, as equation 1 assumes that the KER only results from the potential energy between the two point charges and that there is no additional energy from other sources. The two most important sources of such additional energy are the zero point kinetic energy from the bound state before ionization and the energy transferred during the ionization process by recoil of the escaping electron.

The first is negligible for  $\text{He}_2$ , because the depth of the potential well is only 1 meV. We have also confirmed that by calculating the Coulomb explosion quantum mechanically. We found no difference in the KER between the classical calculation using equation 1 and the quantum calculation which automatically includes the initial state zero point motion (see [25]).

The energy transferred to the two nuclei during the ionization process by the FEL is given by the recoil of the two electrons. The sum momentum distribution of two electrons with a kinetic energy of  $E_\gamma - I_P = 42.4 \text{ eV}$  each was calculated and is reflected in the measured data. For two independent ionization events the distributions of the sum momenta and the momentum difference of

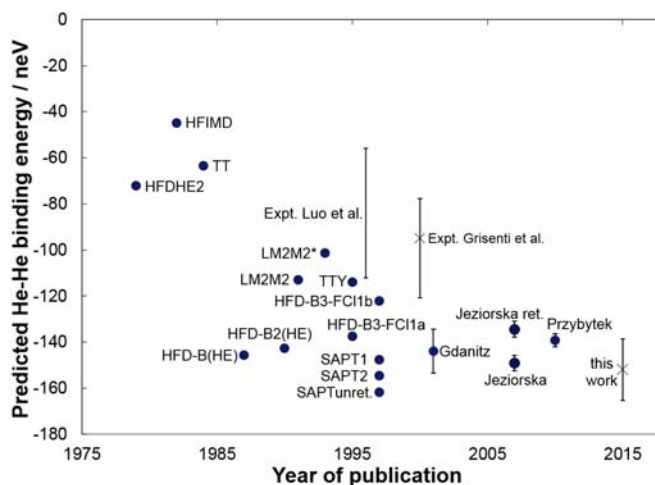


**Fig. 4.** The predicted values for the helium dimer binding energy using various theoretical calculations (HFDHE2[16], HFIMD[17], TT[26], HFD-B(HE)[27], HFD-B2[28], LM2M2[21], LM2M2\*[15], TTY[18], HFD-B3-FC1a[29], HFD-B3-FC1b, SAPT[20, 30], Gdanitz[19], Jeziorska, Jeziorska ret.[31] and Przybytek[5]) are displayed alongside experimental measurements from Luo et al.[10], Grisenti et al.[8] and the present work.

the electrons are equal. While the sum momentum cancels out in the KER calculation the relative momentum adds to it and increases the measured KER. This reduces the slope of the exponential decaying function by 12.1 neV. Taking this into account we obtain a binding energy value of  $151.9 \text{ neV} \pm 1.7(\text{stat}) \pm 10.2(\text{calib}) \pm 1.4(\text{corr}) \text{ neV}$  from our experiment. The statistical error is the error of the fit caused by the statistics of the data points, the calibration error is the uncertainty of the calibration of our COLTRIMS reaction microscope as discussed above and the error labeled (corr) is the estimated error on the correction procedure compensating the detector efficiency and subtraction of random coincidences.

**Comparison with theory.** The exact value of the helium dimer binding energy was subject of dispute for decades. Figure 4 displays the evolution of theoretical predictions as small effects such as deviation from the Born Oppenheimer Approximation, retardation and quantum electrodynamic effects were included into calculations and more computational power became accessible. Our measurement is in good agreement with most recent calculations from Przybytek et al.[5] but cannot distinguish between that and several older calculations[19, 20]. Our obtained results on the  $\text{He}_2$  wavefunction and binding energy provide a new experimental benchmark for theoretical calculations.

**ACKNOWLEDGMENTS.** The experimental work was supported by a Reinhart Koselleck project of the Deutsche Forschungsgemeinschaft. We are grateful for excellent support by the staff of FLASH during our beamtime. We thank R. Gentry and M. Przybytek for providing their theoretical results in numerical form.

1. Riisager K (1994) Nuclear halo states. *Rev. Mod. Phys.* 66:1105–1116.
2. Jensen AS, Riisager K, Fedorov DV, Garrido E (2004) Structure and reaction of quantum halos. *Rev. Mod. Phys.* 76:215–261.
3. Hansen PG, Tostevin JA (2003) Direct reactions with exotic nuclei. *Annu. Rev. Nucl. Part. Sci.* 53:219–261.
4. Tanihata I (1996) Neutron halo nuclei. *J. Phys. G: Nucl Part Phys* 22:157–198.
5. Przybytek M et al. (2010) Relativistic and quantum electrodynamics effects in the helium pair potential. *Phys. Rev. Lett.* 104:183003.
6. Schöllkopf W, Toennies JP (1994) Nondestructive mass selection of small van der waals cluster. *Science* 266(5189):1345–1348.
7. Luo F, McBane GC, Kim G, Giese FC, Gentry WR (1993) The weakest bond: Experimental observation of helium dimer. *J. Chem. Phys.* 98(4):3564–3567.
8. Grisenti RE et al. (2000) Determination of the bond length and binding energy of the helium dimer by diffraction from a transmission grating. *Phys. Rev. Lett.* 85(11):2284–2287.

9. Lin H et al. (2013) Improved determination of the boltzmann constant using a single fixed-length cylindrical cavity. *Metrologia* 50:417–432.
10. Luo F, Giese CF, Gentry WR (1996) Direct measurement of the size of the helium dimer. *J. Chem. Phys.* 104:1151–1154.
11. Cencek W et al. (2012) Effects of adiabatic, relativistic, and quantum electrodynamics interactions on the pair potential and thermophysical properties of helium. *Journal of Chemical Physics* 136:224303.
12. Jagutzki O et al. (2002) Multiple hit readout of a microchannel plate detector with a three-layer delay-line anode. *IEEE Trans. Nucl. Sci.* 49(5):2477–2483.
13. Ullrich J, Moshhammer R, Dorn A, Dörner, R. Schmidt LPH, Schmidt-Böcking H (2003) Recoil-ion and electron momentum spectroscopy: reaction-microscopes. *Rep. Prog. Phys.* 66:1463–1545.
14. Jahnke T et al. (2004) Multicoincidence studies of photon and auger electrons from fixed-in-space molecules using the coltrims technique. *J. Electron. Spectrosc. Relat. Phenom.* 141:229–238.
15. Luo F, Kim G, McBane GC, Giese FC, Gentry WR (1993) Influence of the retardation on the vibrational wave function and binding energy of the helium dimer. *J. Chem. Phys.* 98:9687–9890.
16. Aziz RA, Nain VPS, Carley JS, Taylor WL, McConville GT (1979) An accurate intermolecular potential for helium. *J. Chem. Phys.* 70:4330–4342.
17. Feltgen R, Kirst H, Köhler KA, Pauly H, Torello F (1982) Unique determination of the he2 ground state potential from experiment by use of a reliable potential model. *J. Chem. Phys.* 76:2360–2378.
18. Tang KT, Toennies JP, Yiu CL (1995) Accurate analytical he-he van der waals potential based on perturbation theory. *Phys. Rev. Lett.* 74:1546–1549.
19. Gdanitz RJ (2001) Accurately solving the electronic schrödinger equation of atoms and molecules using explicitly correlated (r12)-mr-ci. vi. the helium dimer (he2) revisited. *Mol. Phys.* 99:923–930.
20. Janzen AR, Aziz RA (1997) An accurate potential energy curve for helium based on ab initio calculations. *J. Chem. Phys.* 107:914–919.
21. Aziz RA, Slaman MJ (1991) An examination of ab initio results for the helium potential energy curve. *J. Chem. Phys.* 94:8047–8053.
22. Kunitzki M et al. (2015) Observation of the efimov state of the helium trimer. *Science* 348:551–555.
23. Lundqvist M, Edvardsson D, Baltzer P, Wannberg B (1996) Doppler-free kinetic energy release spectrum of n22+. *J. Phys. B* 29:1489–1499.
24. Wu J et al. (2013) Strong field multiple ionization as a route to electron dynamics in a van der waals cluster. *Physical Review Letters* 111:083003.
25. Schmidt LPH et al. (2012) Spatial imaging of the h2+ vibrational wave function at the quantum limit. *Phys. Rev. Lett.* 108:073202–1.
26. Tang KT, Toennies JP (1984) An improved simple model for the van der waals potential based on universal damping functions for the dispersion coefficients. *J. Chem. Phys.* 80:3726–3741.
27. Aziz RA, McCourt FRW, Wong CCK (1987) A new determination of the ground state interatomic potential for he2. *Mol. Phys.* 61:1487–1511.
28. Aziz RA, Slaman MJ (1990) An analysis of the its-90 relations for the non-ideality of 3he and 4he: Recommended relations based on a new interatomic potential for helium. *Metrologia* 27:211–219.
29. Aziz RA, Janzen AR, Moldover MR (1995) Ab initio calculations for helium: A standard for transport property measurements. *Phys. Rev. Lett.* 74:1586–1589.
30. Korona T, Williams HL, Bukowski R, Jeziorski B, Szalewicz K (1997) Helium dimer potential from symmetry-adapted perturbation theory calculations using large gaussian geminal and orbital basis sets. *Journal of Chemical Physics* 106:5109.
31. Jeziorska M, Cencek W, Patkowski K, Jeziorski B, Szalewicz K (2007) Pair potential for helium from symmetry-adapted perturbation theory calculations and from supermolecular data. *Journal of Chemical Physics* 127:124303.

DRAFT